Angular Characterization of Polymer Surfaces by FTIR ATR Dichroism with a Rotatable Truncated Hemispheric Crystal

Ping Yuan and Chong Sook Paik Sung*

Institute of Materials Science, Department of Chemistry, University of Connecticut, 97 North Eagleville Road, Storrs, Connecticut 06269-3136

Received February 13, 1991; Revised Manuscript Received June 17, 1991

ABSTRACT: The design and applications of a new attenuated total reflection attachment for an FTIR instrument are described in this paper for the objective of obtaining horizontal angular profiles of IR absorbances from several polymer surfaces. Uniaxially drawn or rolltruded polymers show peanut-shaped angular profiles, when plotted on a full 360° horizontal plane. For poly(ethylene terephthalate), the band at 972 cm^{-1} due to the trans conformer of the ethylene glycol exhibited much greater anisotropy along the draw direction than the band for the gauche conformer at 899 cm^{-1}. Biaxially drawn samples show increasingly larger circles with draw ratio, with the 972-cm^{-1} band showing the greatest increase. The trends observed by IR are generally supported by independent results from X-ray diffraction and birefringence used for the bulk orientation determination. A liquid-crystalline aromatic copolyester made by counterrotating die extrusion exhibits more complex profiles; one surface shows about 45° orientation from the extrusion direction while the opposite surface shows 135° orientation. The surface of rolltruded polypropylene shows very high uniaxial orientation along the extrusion direction.

Introduction

It is well-known that the physical and mechanical properties of polymers are strongly dependent upon molecular orientation, which can be introduced by drawing or extrusion. Such a process changes the structure of the polymer surface as well as the bulk phase, thus affecting the surface properties. Therefore, a basic understanding of the surface structure–properties relationship in polymers demands a detailed and an accurate knowledge of the state of surface molecular orientation. The surface can be defined as representing a depth on the order of microns in many processed polymers such as films or molded parts.

Because of its sensitivity to molecular structural details, infrared spectroscopy by attenuated total reflection (ATR) using a plane-polarized IR beam is a preferred method to probe molecular orientation in a surface depth of a few microns. In IR-ATR dichroism techniques, both the polymer and the polarizer can be rotated by 90°, producing four reflection spectra from which only three spatial absorbencies (A_x, A_y, and A_z) need to be calculated according to the following equations derived by Flournoy and Schaeffers[1]

$$A_{TE_x} = \alpha A_x \tag{1}$$

$$A_{TM_x} = \beta A_y + \gamma A_z \tag{2}$$

$$A_{TE_y} = \alpha A_y \tag{3}$$

$$A_{TM_y} = \beta A_x + \gamma A_z \tag{4}$$

In eqs 1–4, α, β, and γ are the constants determined by the refractive indices of the sample and the crystal and the angle of incidence. The ATR intensities for the transverse electric (TE) and the transverse magnetic (TM) polarization are represented by A_{TE_x} (or A_{TE_y}) and A_{TM_x} (or A_{TM_y}) where the x axis is the draw direction in the case of uniaxial drawing and the y or z axis is parallel or normal to the film plane, respectively.

When the sample is rotated to obtain two reflection spectra, A_{TE_x} and A_{TE_y}, with a standard ATR attachment, the sample must be remounted, resulting in a potentially different optical contact between the crystal and the polymer film. Since ATR intensities change as a function of such a variation in optical contact, the error in dichroic ratios can be substantial. In order to resolve this problem with a standard attachment, a rotatable sample holder with a double-edged reflection crystal has been developed in our laboratory.[2,3] This sample holder, which does not require remounting the sample for sample rotation, has been used to characterize surface molecular orientation and crystallinity on various uniaxially and biaxially drawn polymers, as well as injection-molded liquid-crystalline polymers.[4] More recently, we investigated the relationship between surface structure, topology, and liquid-wetting behavior in oriented polymers by using this sample holder to characterize polymer surface structure.[5]

In using a rotatable holder with a double-edged crystal, it is assumed that equal optical contact is made when the sample is rotated. This assumption is generally valid in many drawn polymers having smooth surfaces. Amorphous polymer films or polymers with low crystallinity fall into this category. However, in highly crystalline polymers such as polypropylene, a high degree of drawing can introduce anisotropic roughness, which may lead to unequal contact in the optical pathways when the sample is rotated. Mirabella proposed a method based on the measurement of band ratios within a single spectrum near a critical angle for such polymers.[6] However, we found that two IR bands at 998 and 973 cm^{-1} (representing crystalline and average orientation, respectively) gave a reasonable trend in the orientation function as a function of draw ratio in drawn polypropylene films.[5]

Face-cut crystals as used in most ATR studies only allow orientation characterization at 0° and 90°, providing a single quantitative measure of orientation. They do not allow characterization at other horizontal angles.

In order to obtain horizontal angular profiles, we have designed a new internal reflection device with a truncated hemispheric crystal and a goniometer which allows a complete horizontal rotation. In this paper, we will show how this goniomer with a new crystal was used to obtain angular profiles of absorbance from the surfaces of several polymers.

0024-9297/91/2224-6095$02.50/0

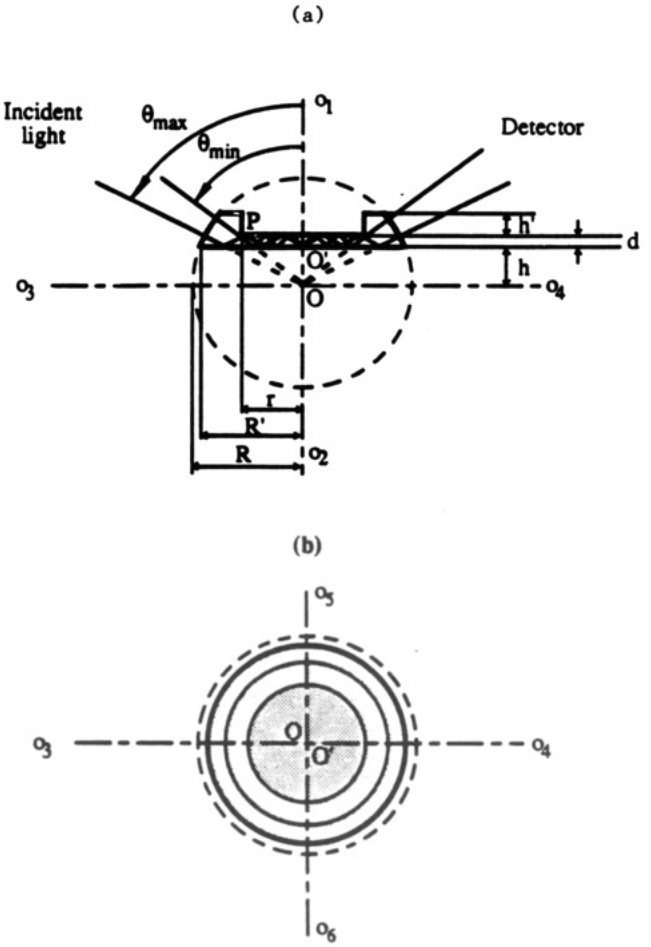

Figure 1. Schematic drawing of the new ATR crystal showing (a) the side view and (b) the top view.

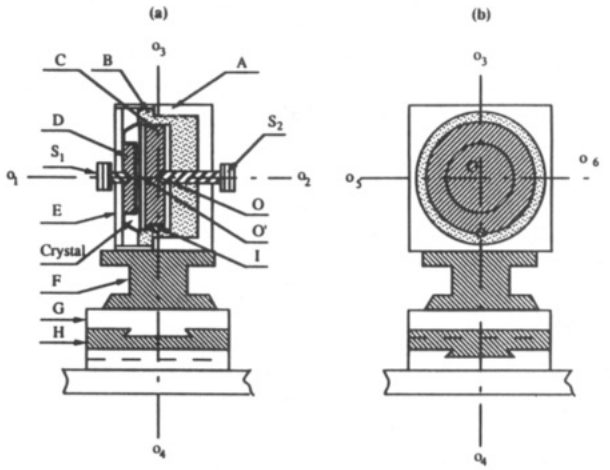

Figure 2. Schematic drawing of the new sample holder showing (a) the side view and (b) the front view.

Experimental Section

ATR Crystal. A schematic drawing of the new ATR crystal is shown in Figure 1. The crystal is made of KRS-5 as a truncated hemisphere to allow multiple reflections, which is more desirable to enhance the spectral intensity in comparison to a hemisphere, allowing only a single reflection. The dimensions of the crystal are chosen so that there will be five reflections on the bottom surface of the crystal regardless of the incident angle, which is limited to from 60° (θ_{min}) to 70° (θ_{max}) as shown in Figure 1. The various dimensions for the crystal are defined in Figure 1.

ATR Sample Holder. Figure 2 illustrates a schematic drawing of both the side view (a) and the front view (b) of the new ATR sample holder. The design of this new ATR sample holder is much simpler and requires less space, in comparison to the previous sample holder for a hemispheric crystal designed by Hobbs in our laboratory.[7] As shown in Figure 2, the truncated hemispheric crystal is held by five pieces of aluminum designated A–E. Piece D is a circular plate with a radius of 15.5 mm, pressing directly on top of the crystal, while piece E is a metal strip which can be attached or detached from piece A. Piece B is a circular piece that fits inside piece A and is rotatable around the o_1–o_2 axis. The crystal sits on the edges of piece B so as to maintain a constant distance between O′ and O. In order to accommodate samples with different thicknesses, a circular plate C is used, by pressing directly on the bottom side of a sample in the case of sample data collection or the crystal in the case of background collection. A small notch I attaches piece C which has a matching groove so as to rotate pieces B and C with the sample. Finally, the piece A fixed with F is rotatable longitudinally around the o_3–o_4 axis. The base plate G or H is designed to be movable along the o_5–o_6 or o_1–o_2 axis, respectively, so that the position of the center O is adjustable. In order to control the clamping pressure with uniform force distribution on the sample, two screws S_1 and S_2 are used with the use of a specific torque wrench. To achieve a uniform force on the sample surface, the strip E is connected with piece A instead of B and the crystal. A problem encountered in the current design was horizontal rotation resistance of the sample holder, which was solved by placing a thin Teflon gasket between pieces B and A. In order to apply enough force to screw S_1, while plate D is able to freely rotate, eight small ball bearings were attached horizontally inside the plate D.

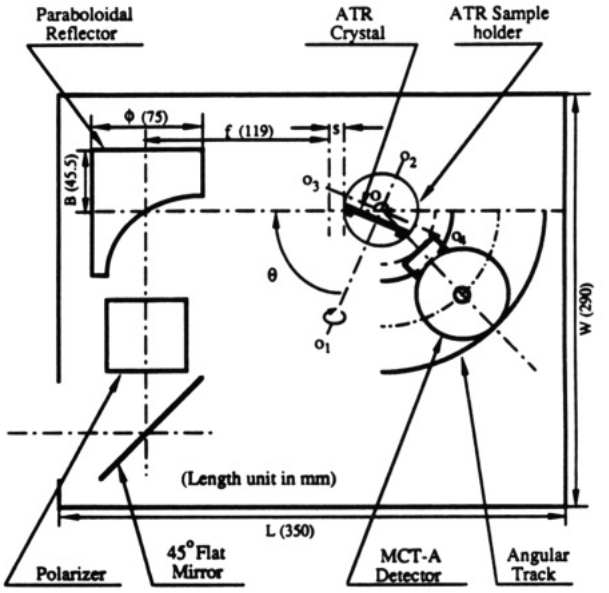

Figure 3. Top view showing the new ATR optical setup in the microsampling compartment of a Nicolet 60 SX FTIR spectrometer.

Optical Setup. Figures 3 and 4 illustrate the schematic drawings of the new optical setup in the microsampling compartment of a Nicolet 60 SX FTIR spectrometer. Figure 3 is a top view with the exact dimensions indicated, while Figure 4 shows the schematic drawing of the optical setup. In this optical arrangement, the main IR beam is directed into the microsampling compartment and reflected by a 45° flat mirror so that it travels parallel to the sample compartment wall before passing through a germanium double-diamond polarizer (PDD-01B from Harrick Scientific Corp.). The collimated beam is focused on a spot which is a small distance (8 mm) away from the ATR crystal entrance by a 90° off-axis parabolic reflector (Melles Griot). The new ATR sample holder is positioned so that the incident beam points to the center of the sphere. The beam enters the crystal with a well-defined incident angle θ and travels inside the crystal without distorting the collimation. The horizontal angular rotation reading is accurate to 1°, since the beam is focused with a parabolic mirror. After reflection from the ATR crystal surfaces, the beam exits from the crystal and refocuses at the same distance (8 mm) away from the exiting surface. A liquid-nitrogen-cooled, mercury–cadmium–telluride (MCT-A) detector is placed near

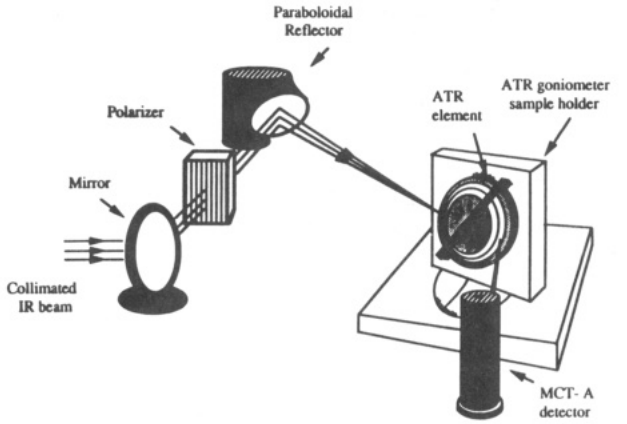

Figure 4. Schematic drawing showing the new ATR optical arrangement.

the exiting focal point. While horizontal angle changes do not require the position of the detector to be changed, its position has to be moved when the incidence angle is changed. Therefore, the detector is mounted on an angular track, as shown in Figure 4.

Materials. Undrawn, uniaxially drawn, and biaxially drawn poly(ethylene terephthalate) (PET) films were chosen for the purpose of testing the new optical system since their surface and bulk structures are well characterized. These PET samples were kindly provided by Mr. H. Y. Lee of SKC, Ltd., Korea. The uniaxially drawn PET films were prepared by stretching the original undrawn sheets at 90 °C at a strain rate of 3 cm/min. The biaxially drawn films were prepared under the same drawing temperature and speed with simultaneous stretching along x and y directions of the sample films. The intrinsic viscosity of the PET film is 0.56 dL/g in a solution of 60:40 wt % phenol–tetrachloroethane at 30 °C. The surface of these PET samples was found to be smooth in the scale of 2 μm by a Talysurf profilometer.

A film of a thermotropic aromatic copolyester consisting of 73 mol % p-hydroxybenzoic acid (HBA) and 27 mol % 6-hydroxy-2-naphthalic acid (HNA) was processed by a counterrotating die extrusion by Foster-Miller Co. In this process, molten polymer is fed into the space between two counterrotating dies, followed by blowing and stretching.

The last set of samples were polypropylene films kindly provided by Prof. Magill of the University of Pittsburgh. These samples were prepared by a process called rolltrusion which involves simultaneous rolling and extrusion rather than a conventional two-step process of drawing followed by rolling. The number- and weight-average molecular weights of the samples are known to be 65 600 and 413 000, respectively. One set of samples were rolltruded at 150 °C with a draw ratio of 5.6 or 9.0, while another sample was rolltruded at 160 °C with a draw ratio of 18.0.

Angular Profiles of Surface Absorbance by Polarized FTIR-ATR. The ATR crystal was cleaned by dipping in xylene followed by blow drying with argon and carefully wiping with a nonabrasive optical lens tissue, until the background spectrum was satisfactory. When sample was placed between the crystal and the plate C of the sample holder, the pressure applied to ensure consistently good contact was carefully chosen so that it would not be too strong to cause distortion of the spectra nor too weak that it reduces the spectrum quality. The applied forces on the torque wrench on screw S_1 and screw S_2 were 20 and 80 in. oz, respectively, for all the samples. The FTIR signal intensity from a Nicolet 60SX spectrometer using this ATR setup was 3 times stronger than that with a face-cut parallelogram crystal used in our earlier work.[4] An incident angle of 60° was used with a total number of 320 scans at each horizontal angle. The sample spectra, as well as the background spectra were collected at every 30° intervals through the full angular range of 0–360°. Sample spectra were divided by the background spectra corresponding to each polarization and angle. Spectra with a resolution of 2 cm^{-1} were obtained, and peak heights with the local base lines were used for intensity measurements.

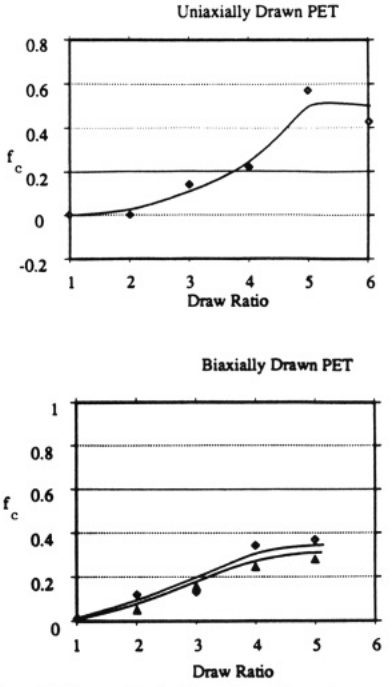

Figure 5. Crystalline orientation function, f_c, as a function of the draw ratio as determined from X-ray diffraction, in uniaxial and biaxial PET films. For biaxial samples, data points (–◇–) or (–△–) represent f_c along the x direction or the y direction, respectively.

X-ray Diffraction Measurements. In order to complement the FTIR-ATR dichroism techniques, the wide-angle X-ray diffraction (WAXD) method was used as an independent method for the crystalline orientation determination of bulk PET samples. A Rigaku "Rotoflex" Ru-200B series X-ray diffractometer was used at room temperature using graphite-filtered monochromatic Cu Kα radiation (30 kV, 80 mA), which has a wavelength of 1.5418 Å. The sample strips (1 mm in width × 2 cm in length) were placed with the draw direction perpendicular to the incident beam. The distance between the sample strip and the detector was set to be 90 mm, and the WAXD intensity was detected with a Nicolet area detector. The WAXD image was analyzed and displayed using the "polygraf" software program developed at the University of Connecticut by Dr. J. Gromek.[8]

Birefringence Measurements. As another independent method of obtaining information on the overall orientation rather than the crystalline orientation of bulk PET samples, a birefringence measurement was carried out with an Erhinghaus rotary compensator, using sample strips cut into 5 mm × 10 mm sizes.

Results and Discussion

1. Characterization of Orientation in Bulk PET Films by X-ray Diffraction and Birefringence. The crystalline orientation function f_c was obtained from the azimuthal scans of the diffracted X-ray intensity, I_ϕ, from the (100) plane by using the following three equations which are applicable for the crystal structure of PET, as used by Heffelfinger and Burton.[9]

$$\cos^2 \phi_{100} = \frac{\int I(\phi) \sin \phi \cos^2 \phi \, d\phi}{\int I(\phi) \sin \phi \, d\phi} \tag{5}$$

$$\cos^2 \phi_c = 1 - 2\langle \cos^2 \phi_{100} \rangle \tag{6}$$

$$f_c = \frac{3\langle \cos^2 \phi_c \rangle - 1}{2} \tag{7}$$

Figure 5 shows the plot of the crystalline orientation

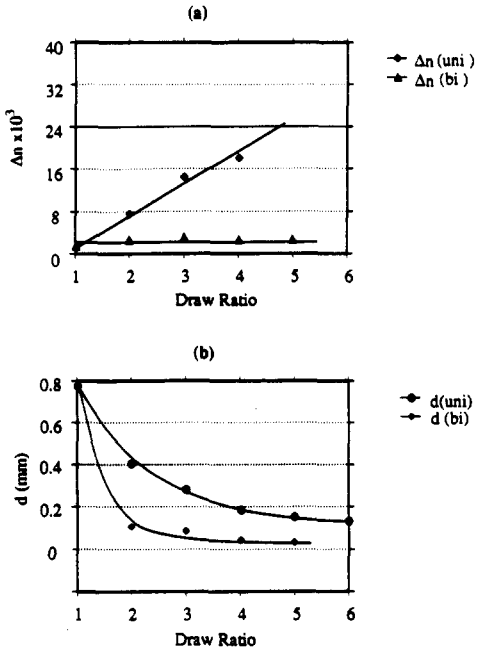

Figure 6. (a) Birefringence (Δn) and (b) the film thickness as a function of the draw ratio of uniaxial and biaxial PET films.

function, f_c, as a function of the draw ratio for uniaxially or biaxially drawn PET samples. For both sets of samples, an increase in orientation is observed as the draw ratio is increased from an almost zero value for the unoriented sample to about 0.5 or 0.4 for 5 times the uniaxially or biaxially drawn samples, respectively. For biaxially drawn samples, f_c along either draw direction is similar, indicating balanced planar orientation. These results clearly indicate the presence of increasing crystalline orientation in the bulk in the drawn PET films.

The birefringence, Δn ($=n_x - n_y$), is plotted in Figure 6a, while the changes in film thickness are plotted in Figure 6b, for both uniaxially and biaxially drawn PET samples. Clearly, the thickness decreases more for these balanced biaxial samples than for the uniaxial samples. The birefringence for uniaxial samples increases with draw ratio, indicating overall orientation along the draw direction (x) in comparison to the perpendicular y direction on the film surface. The birefringence for biaxial samples remains very low and constant in regards to these two film surface directions since they are well balanced. In these biaxial samples, the birefringence, Δn ($=n_x - n_z$), would be expected to show an increase with draw ratio.

2. Characterization of Bulk Crystallinity by Thermal Analysis. Bulk crystallinity was measured by thermal analysis assuming the heat of fusion (ΔH) for 100% crystallinity to be 27 cal/g.[10] Figure 7 shows the plot of the heat of fusion and the degree of bulk crystallinity as a function of the draw ratio for PET samples. For uniaxial samples, the degree of crystallinity starts out at about 34% and gradually increases to about 41% as the draw ratio increases to 6. For biaxial samples, a similar increase in crystallinity is achieved at a lower draw ratio of 3 × 3 and only a slight increase is indicated beyond that draw ratio.

3. Angular Profile of IR Absorption on PET Surfaces by FTIR-ATR Technique. Figure 8 shows four IR-ATR spectra obtained from the surface of a 5 × 1 uniaxially drawn PET film by a 30° increment starting from the draw direction (0°) to the transverse direction using a 60° incident angle with a TE polarization. Since a 60° incident angle is well above the critical angle ($\theta_c \simeq$ 43°) for the KRS-5 crystal, the spectra is free from

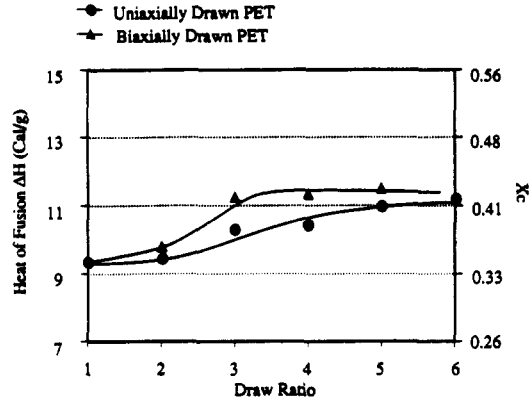

Figure 7. Heat of fusion (ΔH) and bulk crystallinity as a function of the draw ratio for uniaxial and biaxial PET films.

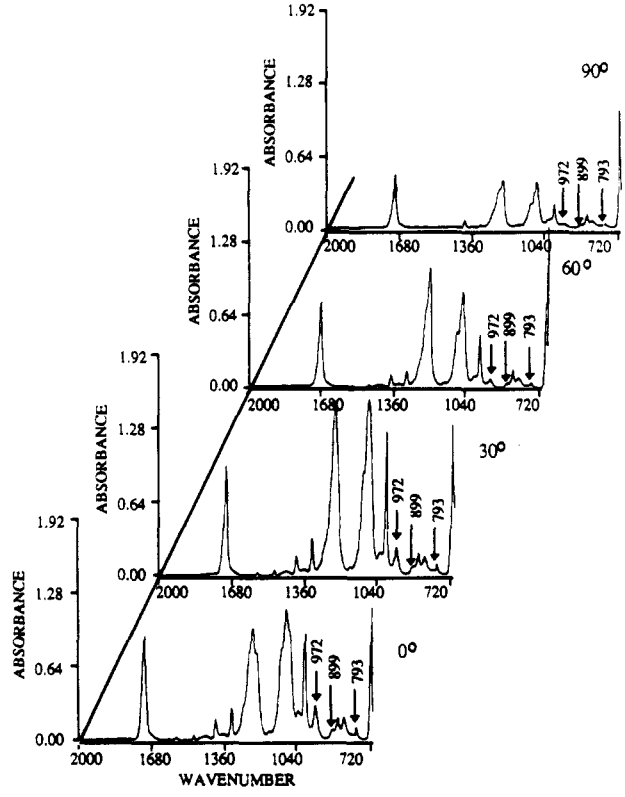

Figure 8. FTIR-ATR spectra for 5 × 1 uniaxially drawn PET films as a function of horizontal angles using 60° incident angle with TE polarization. The draw direction (x) corresponds to 0°, while 90° is transverse to the draw direction.

distortion. Under these experimental conditions, the depth of penetration probed by TE polarization is about 1.2 μm at 1000 cm^{-1}. We used three parallel bands at 793, 899, and 972 cm^{-1} to obtain angular profiles after expanding the spectra in these regions and obtaining peak heights from local base lines. The band at 795 cm^{-1} is associated with the vibrations of the benzene ring of PET and may be used as an indication of an overall chain orientation. The bands at 972 and 899 cm^{-1} have been assigned to the trans and gauche conformer of the ethylene glycol unit of PET, respectively.

Qualitatively, it is noted that the peak intensities, particularly for the 972-cm^{-1} peak, decrease sharply as the angle is changed from 0, 30, 60 to 90°, indicating anisotropy due to orientation. The measured angular profiles of IR-ATR intensity, A_{TE}, can be plotted on two-dimensional polar charts to provide a visual display of the anisotropy. Figures 9a, 10a, and 11a illustrate such profiles for three selected IR bands for uniaxially drawn PET

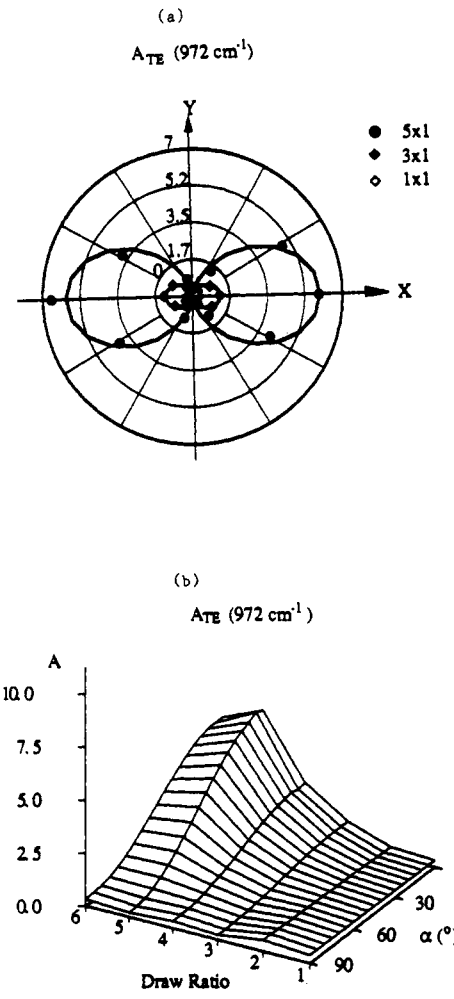

Figure 9. (a) Angular profiles and (b) three-dimensional plot of IR absorbance, A_{TE}, at 972 cm^{-1} for uniaxially drawn PET films.

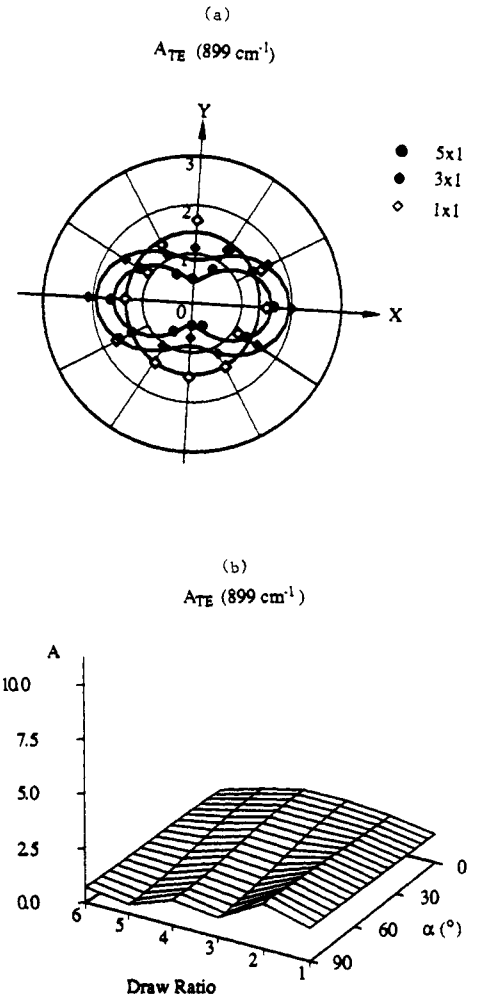

Figure 10. (a) Angular profiles and (b) three-dimensional plot of IR absorbance, A_{TE}, at 899 cm^{-1} for uniaxially drawn PET films.

samples. For an unoriented sample, the absorption intensities would be the same at all angles, resulting in a circle. This is found to be the case for all three bands. For uniaxially drawn samples, all the band profiles show peanut-shaped profiles with an anisotropy along the draw direction (x). Such an anisotropy is most pronounced with the 972-cm^{-1} band. For example, the dichroic ratio between $A_{TE,0}$ and $A_{TE,90}$ for 972 cm^{-1} can be almost 20 for the 5 × 1 drawn sample. This dichroic ratio corresponds to a high value of the orientation function of 0.86. For a band at 793 cm^{-1}, a modest increase in the dichroic ratio from 1 to about 2.5 is observed with increasing draw ratio, corresponding to an orientation function of 0.33. However, the intensity of the 899-cm^{-1} gauche band behaves quite differently from that of the trans band. Along the draw direction, it increases first and then decreases after passing a maximum intensity value. A continued large increase in anisotropy in the 972-cm^{-1} band and a slight decrease in 899 cm^{-1} after reaching a maximum are attributable to the conversion of some gauche units to trans units as well as better orientation and/or crystallization of trans with increasing draw ratio, as shown by thermal analysis. The behavior of the gauche peak at 899 cm^{-1} may be due to the initial orientation which increases anisotropy, followed by the conversion of some gauche units to trans units at high draw ratio, resulting in a decrease in the absorption intensity. As another way to illustrate the behavior of these bands, the IR intensities, A_{TE}, are plotted on three-dimensional plots as a function of the horizontal angle from 0 to 90° and the draw ratio as shown in Figures 9b, 10b, and 11b. In these diagrams, the data for 2 × 1, 4 × 1, and 6 × 1 samples are also included. Since the angular profiles are symmetrical for every 90° in these samples, we chose to plot only from 0 to 90°. In these three-dimensional plots, a straight horizontal line along the angles indicates isotropy as in case of undrawn samples. The trends observed with a two-dimensional plot are also seen in these three-dimensional plots.

For biaxially drawn PET samples, the A_{TE} intensity as a function of horizontal angles on the surface of the film is displayed in Figures 12a, 13a, and 14a for three bands. These samples were prepared by simultaneous stretching along x and y directions. It can be seen that the angular profiles of IR bands at all three bands become more circular with the draw ratio. This indicates a tendency of reasonably well-balanced molecular chain orientation along all directions in the surface plane of the film due to simultaneous biaxial drawing. Three-dimensional plots including all the biaxially drawn samples are illustrated in Figures 12b, 13b, and 14b. While the angular profiles are mostly independent of horizontal angles for all the bands, there are differences in the absolute intensities of the absorbances as a function of draw ratio. For example, the intensity of the 972-cm^{-1} band for the trans conformer increases sharply with increasing draw ratio as illustrated in Figure 12a. From undrawn to 5 × 5 times the drawn sample, the intensity increases about 10 times at all angles. In contrast, the intensity at the 899-cm^{-1} gauche band changes little when biaxially drawn either 3 × 3 times or 5 × 5 times. The benzene ring band at 793 cm^{-1} shows a

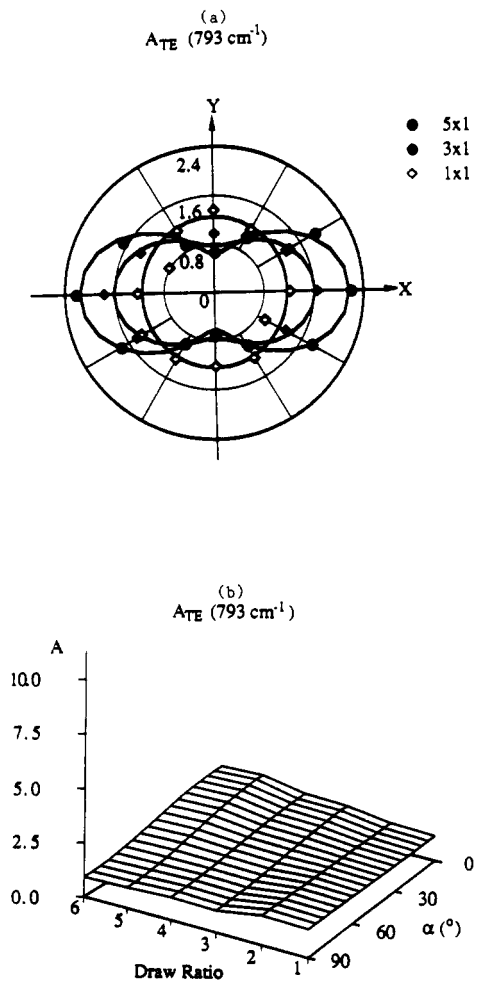

Figure 11. (a) Angular profiles and (b) three-dimensional plot of IR absorbance, A_{TE}, at 793 cm^{-1} for uniaxially drawn PET films.

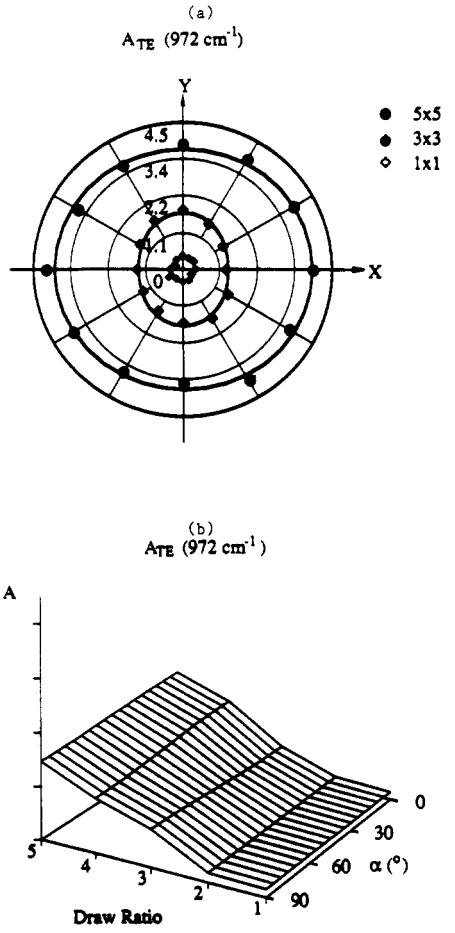

Figure 12. (a) Angular profiles and (b) three-dimensional plot of IR absorbance, A_{TE}, at 972 cm^{-1} for biaxially drawn PET films. X and Y are draw directions.

moderate increase (about 1.7 times) when drawn to 5 × 5 times. It can be pictured that the molecular chains are extended and aligned by uncoiling in both the transverse and machine directions due to the elongation of the sample by biaxial stretching. The greatest change in structure must have occurred in the thickness direction because both the machine and transverse directions are expanding. This is confirmed by an increase in the dichroic ratio D_{xz} upon biaxial drawing. The dichroic ratio D_{xz} at 795 cm^{-1} for the 5 × 5 biaxially drawn sample is found to be about 12, corresponding to an orientation function of 0.78. For the calculation of D_{xz}, the values of α, β, and γ of 3.29, 1.47, and 3.90 were used, respectively. Due to the change in thickness, the chains would be against each other, producing a chain alignment parallel to the surface which led to crystallization with the crystal parallel to the surface. Because of the chain entanglement, chains in both trans and gauche forms tend to line up parallel to the surface under the simultaneous biaxial stretching field. This would cause an increase in intensity for both the 972- and 899-cm^{-1} bands with the draw ratio. However, the conversion of the gauche isomer to the trans isomer, together with the conversion of the amorphous trans to the crystalline trans, would result in an intensity increase of the 972-cm^{-1} band in the xy surface plane and a relatively little change of the 899-cm^{-1} band. The thermal analyses confirmed an increase in the degree of crystallinity as a function of biaxial drawing.

4. Angular Profile of IR Absorption on Liquid-Crystalline Copolyester Surfaces Extruded by Counterrotating Die. The IR-ATR spectra of a HBA/HNA (73/27) copolyester is shown in Figure 15, representing the outside of the film after extrusion by a counterrotating die. Two bands at 1473 and 1507 cm^{-1} are chosen for the angular dependence, since they are known to be parallel bands associated with the skeletal vibrations of the benzene and naphthalene rings in the polymer.[11] The band at 1473 cm^{-1} is due to the HNA component while the band at 1507 cm^{-1} is mostly due to HBA with some contribution from HNA. An interesting angular dependence is observed in Figure 15 for these two bands. For example, the intensities at 120° and 300° appear to be the strongest among all the horizontal angles. The solid lines in Figure 16 shows the angular distributions of IR absorbance (A_{TE}) based on Figure 15, clearly exhibiting a biaxial orientation centered around 135° from the extrusion direction (x). The dotted lines represent the angular profile of the inside of the film, showing a biaxial orientation centered around 45° from the extrusion direction. It is assumed that the inside and outside profiles of the film are results of counterrotating flow and subsequent orientation with this rigid liquid-crystalline polymer. The differences in absorbance values for the inside and the outside of the films might be due to a difference in the surface optical property of each side. The outside of the film was relatively shiny and smooth in comparison to the inside of the film, thus leading to higher absorbances for the outside.

In order to confirm that these profiles are real, the same copolyester drawn uniaxially was tested using the same two bands. Figure 17 shows the results on the uniaxial sample (in dotted lines) in comparison to the outside of the counterrotating die extruded film as indicated by solid

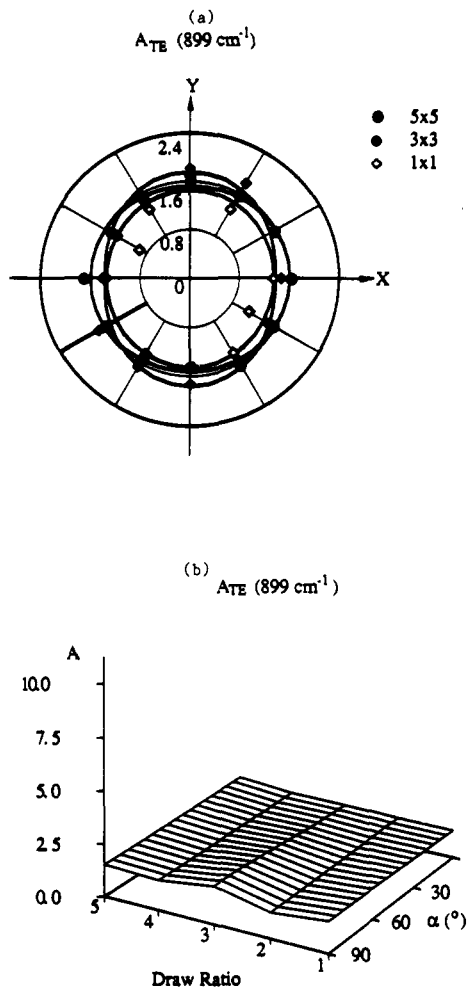

Figure 13. (a) Angular profiles and (b) three-dimensional plot of IR absorbance, A_{TE}, at 899 cm^{-1} for biaxially drawn PET films. X and Y are draw directions.

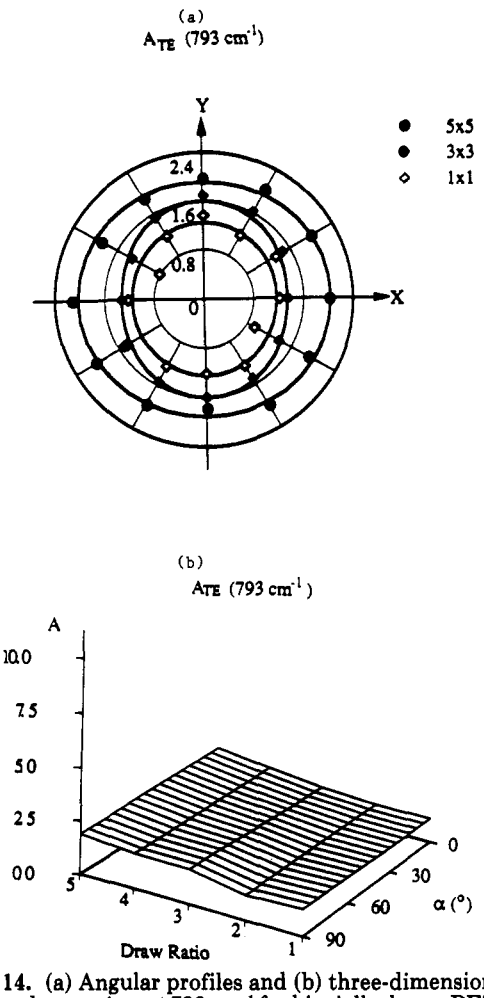

Figure 14. (a) Angular profiles and (b) three-dimensional plot of IR absorbance, A_{TE}, at 793 cm^{-1} for biaxially drawn PET films. X and Y are draw directions.

lines. The profiles for the uniaxial sample are as expected from the PET results, as indicated in Figure 9. Therefore, we conclude that the profiles in Figure 16 are truly representative of the surface biaxial orientation present on copolyester films produced by counterrotating die extrusion. In fact, Farrell and Fellers reported recently that such a process can produce similar biaxial orientation when liquid-crystalline (hydroxypropyl)cellulose was used.[12] They were able to move the chain orientation from the extrusion direction in the absence of counterrotation to almost the transverse direction, depending on the speed of the rotation. Our results are in agreement with the observations based on fibril structure.[13] Throughout the thickness of the film, we expect the orientation to be between 45° and 135° due to different shear fields imposed on the sample during processing.

5. Angular Profile of IR Absorption on Rolltruded Polypropylene Surfaces. Rolltrusion is a single-pass process involving a simultaneous rolling and extrusion and has been demonstrated as an effective method for producing transparent, high-modulus, and high-strength plastics by Magill and co-workers.[14] It was also proposed that the morphology of rolltruded polymers may be triaxial rather than uniaxial. In other words, while the orientation is expected to be the greatest along the extrusion direction (x), Magill et al. found that the orientation along the y and z directions may not be the same. For example, they found that the modulus in the draw direction has been improved by almost 30 times, while it was improved only 3 times in the other direction, when rolltruded at 125 °C for polypropylene. In order to examine if such a model of triaxial orientation can be detected on polymer surfaces, IR absorbances on the surfaces of rolltruded polypropylene films were measured as a function of the horizontal angles for both transelectric (TE) and transmagnetic (TM) polarizations.

For polypropylene, two absorption bands at 998 and 973 cm^{-1} are used. Both bands show parallel dichroism with the 998-cm^{-1} band mostly in the crystalline phase while the 972-cm^{-1} band is known to be in both the crystalline and amorphous phases. Therefore, the orientation functions of the 972-cm^{-1} band can be used to represent the average chain orientation while those of the 998-cm^{-1} band represent the crystalline phase. Figure 18 shows the angular profiles of the IR absorbance (A_{TE}) at 998 cm^{-1}. Increasing anisotropy along the extrusion direction is clearly seen in the peanut-shaped profiles as the draw ratio increases. Values of α, β, and γ for the eqs 1–4 are determined to be 2.28, 1.22, and 2.63, respectively, using an average value of the refractive index of 1.51 for the polypropylene samples. All the angular data of TE and TM polarization are used to determine the average value of the absorbance along the z direction, $\bar{A}_z$

$$\bar{A}_z = \frac{\sum A_{TM} - \frac{\beta}{\gamma}\sum A_{TE}}{n\gamma} \tag{8}$$

where n is the number of angular data used. When the average of all the angular data is taken to obtain $\bar{A}_z$, any effect of surface roughness is minimized. The absorbances in x, y, and z directions are listed in Table I for several

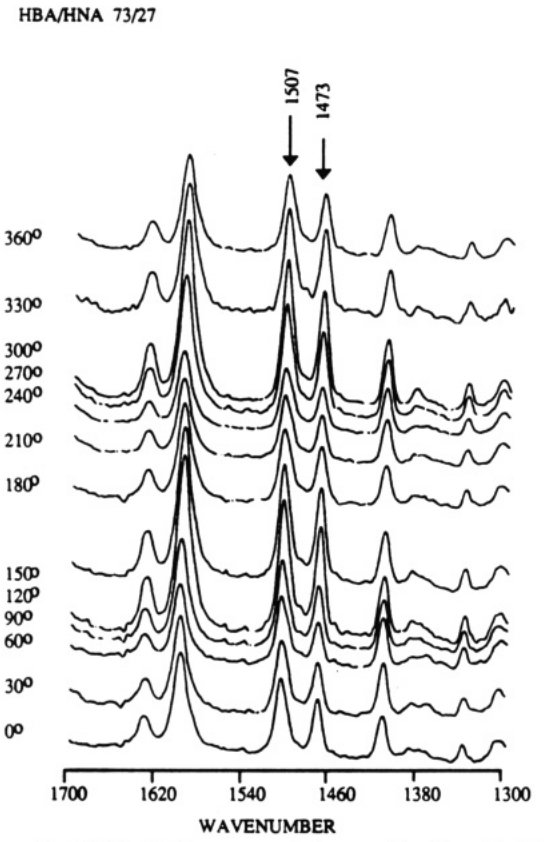

Figure 15. FTIR-ATR spectra of the outside film of a HBA/HNA (73/27) copolyester extruded by counterrotating die. The extrusion direction is along 0°.

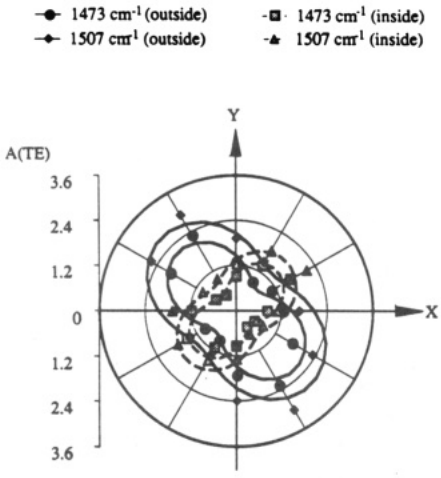

Figure 16. Angular profiles of IR absorbance, A_{TE}, on the outside surface (solid line) and the inside surface (dotted lines) of a HBA/HNA (73/27) copolyester extruded by counterrotating die for two parallel bands at 1473 and 1507 cm^{-1}.

rolltruded samples as well as an undrawn control sample. After rolltrusion, the A_x values are much greater than A_y or A_z values, implying that the chains are mostly oriented toward the draw direction. In fact, it is noted that the orientation function quickly increases to almost unity for both the crystalline and average band for highly drawn samples. By birefringence measurements, the amorphous and crystalline orientation functions of the rolltruded polypropylene samples were found to approach unity also by Magill et al.[14b] However, comparison of A_y and A_z values indicates only a small difference, implying an absence of the preferential orientation along the y or z direction on the surface of these samples. In other words, we do not observe substantial evidence of triaxial orientation in these

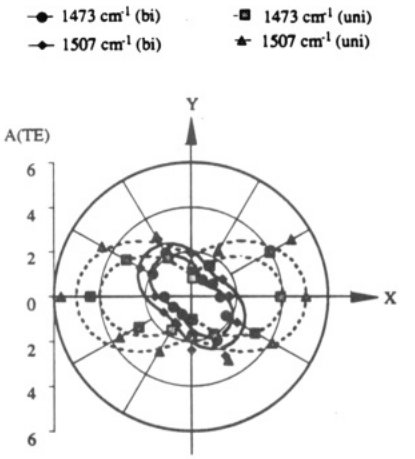

Figure 17. Comparison of the angular profile of IR absorbance of the outside surface of counterrotating die extruded (solid lines) film with that of a uniaxially drawn film surface (dotted lines) of HBN/HNA (73/27).

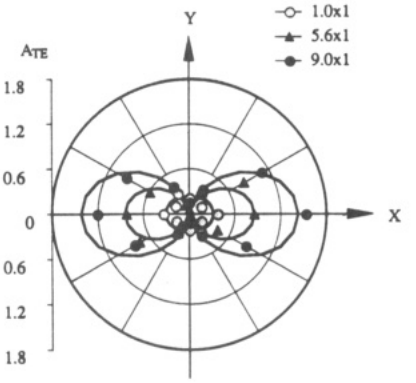

Figure 18. Angular profiles of IR absorbance, A_{TE}, at 998 cm^{-1} for rolltruded polypropylene samples.

Table I
Three Spatial Absorbances and Orientation Function[a] for Rolltruded Polypropylene for the 977- and 998-cm^{-1} IR Bands

draw ratio	draw temp, °C	A_x	A_y	A_z	f_{xy}[a]
	977-cm^{-1} Band				
undrawn		0.14	0.10	0.07	0.11
5.6	150	0.37	0.02	0.05	0.85
9.0	150	0.67	0.06	0.03	0.77
18	160	0.53	0.01	0.01	0.95
	998-cm^{-1} Band				
undrawn		0.07	0.04	0.06	0.20
5.6	150	0.35	0.03	0.05	0.78
9.0	150	0.62	0.03	0.01	0.87
18	160	0.50	0.01	0.01	0.94

[a] $f_{xy} \equiv (D_{xy} - 1)/(D_{xy} + 2)$ where $D_{xy} = A_x/A_y$.

samples, when probed for the first few microns. Instead, they appear to be mostly uniaxially oriented. This trend in the surface does not necessarily mean the absence of triaxial orientation in the bulk.

Summary

In this paper, we describe the development of a new attenuated total reflection attachment for an FTIR instrument and its application to obtain horizontal angular profiles of IR absorbances from several polymer surfaces. The new optical setup capable of five internal reflections with well-defined incidence angles allows a full 360° rotation horizontally. Several polymer samples were used to demonstrate the capability of this attachment. First, films of undrawn, uniaxially drawn, and biaxially drawn

poly(ethylene terephthalate) (PET) were characterized using three IR bands at 972, 899, and 793 cm^{-1}. For uniaxially drawn PET, all the band intensities show peanut-shaped angular profiles, when plotted on a full 360° horizontal plane. The band at 972 cm^{-1} due to the trans conformer of the ethylene glycol unit exhibited much greater anisotropy along the draw direction than the band for the gauche conformer at 899 cm^{-1}. For biaxial PET, the angular profiles of the band intensity become larger circles with an increasing draw ratio, with the 972-cm^{-1} band showing the greatest increase. Independent results from X-ray diffraction and birefringence for the bulk structure support the general trends observed for the PET surfaces by the IR technique. As examples of samples with a more complicated processing history, a liquid-crystalline aromatic copolyester (LCP) made by counterrotating die extrusion and rolltruded polypropylene (PP) samples were also investigated. The angular profiles of LCP polymer surfaces show about 45° orientation from the extrusion direction on one surface while the opposite surface shows 135° orientation. The surfaces of PP samples show very high uniaxial orientation along the extrusion direction.

Acknowledgment. This work was in part supported by the Office of Naval Research. We are grateful for the polymer samples provided by SKC, Ltd., of Korea, Foster-Miller Co., and Professor Magill of the University of Pittsburgh.

References and Notes

(1) Flournoy, P. A.; Schaeffers, W. J. *Spectrochim. Acta* **1966**, *22*, 5.
(2) Sung, C. S. P. *Macromolecules* **1981**, *14*, 591.
(3) Hobbs, J. P.; Sung, C. S. P.; Krishnan, K.; Hill, S. *Macromolecules* **1983**, *16*, 193.
(4) Pirnia, A.; Sung, C. S. P. *Macromolecules* **1988**, *21*, 2699.
(5) Sung, N. H.; Lee, H. Y.; Yuan, P.; Sung, C. S. P. *Polym. Eng. Sci.* **1989**, *29*, 791.
(6) Mirabella, F. M. *Spectroscopy* **1990**, *5*, 20.
(7) Sung, C. S. P.; Hobbs, J. P. *Polym. Prepr. (Am. Chem. Soc., Div. Polym. Sci.)* **1984**, *25*, 154.
(8) Gromek, J. M.; Saini, A. R.; Azaroff, L. V., presented at the American Crystallographers Association Annual Meeting, Toledo, OH, July 1991.
(9) Heffelfinger, C. J.; Burton, R. L. *J. Polym. Sci.* **1960**, *47*, 289.
(10) Polymer Handbook, 2nd ed.; Brandrup, J., Immergut, E. H., Eds.; Wiley: New York, 1975; p V-73.
(11) Ouchi, I.; Hosoi, M.; Shimotsuma, S. *J. Appl. Polym. Sci.* **1977**, *21*, 3445.
(12) Farrell, G. W.; Fellers, J. F. *J. Polym. Eng.* **1986**, *6*, 263.
(13) Rubin, L. (Foster-Miller Co.) Personal communication, 1990.
(14) (a) Voss, H.; Friedrich, K.; Magill, J. H. *J. Appl. Polym. Sci.* **1987**, *34*, 177. (b) Magill, J. H.; Sun, D. C.; Shankernarayanan, M. J. *J. Appl. Polym. Sci.* **1987**, *34*, 2337. (c) Sun, D. C.; Magill, J. H. *J. Polym. Sci., Part C: Polym. Lett.* **1989**, *27*, 65. (d) Sun, D. C.; Berg, E. M.; Magill, J. H. *Polym. Eng. Sci.* **1990**, *30*, 635.

Registry No. PET, 25038-59-9; (HBA)(HNA) (copolymer), 81843-52-9; polypropylene, 9003-07-0.